Kybernetika

Eduardo Ruiz Velázquez; Oscar D. Sánchez; Griselda Quiroz; Guillermo O. Pulido

Parametric Identification of Sorensen model for glucose-insulin-carbohydrates dynamics using evolutive algorithms

Terms of use:

PARAMETRIC IDENTIFICATION OF SORENSEN MODEL FOR GLUCOSE-INSULIN-CARBOHYDRATES DYNAMICS USING EVOLUTIVE ALGORITHMS

Eduardo Ruiz Velázquez, Oscar D. Sánchez, Griselda Quiroz and Guillermo O. Pulido

Diabetes mellitus (DM) is a disease affecting millions of people worldwide, and its medical care brings an economic wear to patients and public health systems. Many efforts have been made to deal with DM, one of them is the full-automation of insulin delivery. This idea consists in design a closed-loop control system to maintain blood glucose levels (BGL) within normal ranges. Dynamic models of glucose-insulin-carbohydrates play an important role in synthesis of control algorithms, but also in other aspects of DM care, such as testing glucose sensors, or as support systems for health care decisions. Therefore, there are several mathematical models reproducing glycemic dynamics of DM, most of them validated with nominal parameters of standardized patients. Nevertheless, individual patient-oriented models could open the possibility of having closed-loop personalized therapies. This problem can be addressed through the information provided by open-loop therapy based on continuous glucose monitoring and subcutaneous insulin infusion. This paper considers the problem of identifying particular parameters of a compartmental model of glucose-insulin dynamics in DM; the goal is fitting the model response to historical data of a diabetic patient collected during a time period of her/his daily life. At this time, Sorensen model is one of the most complete compartmental models representing the complex dynamics of the glucose-insulin metabolism. This is a system of 19 ordinary differential equations (ODEs), thus the identification of its parameters is a non-easy task. In this contribution, parameter identification was performed via three evolutionary algorithms: differential evolution, ant colony optimization and particle swarm optimization. The obtained results show that evolutionary algorithms are powerful tools to solve problems of parametric identification. Also, a comparative analysis of the three algorithms was realized throw a wilcoxon sign-rank test, in which colony optimization had the better performance. The model obtained with the estimated parameters could be used to in type 1 diabetes mellitus (T1DM) care, such as in the design of full-automation of insulin infusion.

Keywords: dynamic model of insulin-glucose, identifiability, parameter estimation, evolutionary algorithms, differential evolution, ant colony optimization, particle swarm optimization

Classification: 93B30, 93B40

1. INTRODUCTION

Diabetes mellitus is a metabolic disorder characterized by increased levels of blood glucose (hyperglycemia), which is caused by a deficit in the secretion or a defect in the action of the insulin hormone. This hormone is produced in pancreas and it controls the level of glucose in blood, so it is essential for our metabolism. Uncontrolled DM care can lead to complications such as nerve and brain damage, heart diseases, vision loss, amputations, kidney diseases and ultimately death [16]. Nowadays DM is a critical public health problem being one of the leading causes of death. Just in 2014 it was estimated that approximately 422 million adults were living with diabetes [40].

A particular type of this disease is caused by an immunological fault blocking pancreatic insulin production, this is called type 1 diabetes mellitus (T1DM). The conventional treatment of T1DM consists in injections of exogenous insulin to regulate glucose glycemic values. Nevertheless, the regulation is difficult to perform due to the complexity of the glucose metabolism and its main disturbances: meal, stress, exercise, among others [36]. The automation glucose control has been for a long time an objective to develop the called artificial pancreas, this is, a closed-loop system to automate insulin infusion by means of a continuous glucose monitoring and an insulin pump (see [19] – [21] and [7]).

With the purpose of designing a control algorithm to connect the insulin pump and glucose monitoring system, it is necessary a dynamic model of glucose-insulin-carbohydrates [11]. This could be useful, for example, to verify the effectiveness of control before clinical trials , that is, to carry out in silico assessments. Different dynamic models has been reported in literature, among them, we can mention the model of Bergman et al., which is the simplest one and it was developed for patients with T1DM in intensive care [6]. It reproduces the systemic dynamics of glucose and insulin, thus important physiological processes are not considered. Hovorka et al. proposed a compartmental model of three subsystems: glucose, insulin and insulin action [25]. Wilinska et al. presented a model to assess the delivery of insulin in patients with T1DM [39]. On the other hand, there are approaches considering physiological aspects not only systemic response of glucose metabolism. Tiran et al. developed a model of the dynamics of glucose [35], Guyton et al. [22] followed the line of Tiran et al. and they presented a model of the metabolism of insulin-glucose in healthy individuals. Such model was also used by Cobelli et al. to derive an integrated whole-body model [29]. Adopting some features of various models, Sorensen developed a compartment model to represent the major organs that interact in glucose-insulin dynamics [34]. These organs are: brain, heart, lungs, intestine, liver, kidney and periphery. The methodology proposed by Sorensen includes the mass balance of glucose and insulin at each compartment, and it results in a system of 19 ODEs.

A critical issue of physiological models is the parametric identification both single-subject models or a nominal model describing a study population [8]. The access to measured signals on a physiological process can be restricted, thus the parametric estimation of a model becomes an interesting problem [23]. This could be addressed if some states of the proposed model can be measured. In the case of the model of Sorensen, the parametric identification is not a simple task due to the large number of parameters.

The task of parametric identification in physiological models for T1DM has been

performed to represent different scenarios of this disease, such as the work presented in [23]; in there they build on a nonlinear physiologically motivated time-varying model of glucose regulation. They adopted the bayesian approach to estimate model parameters and to obtain posterior probability distribution of time-invariant and time-varying parameters with the use of Markov chain Monte Carlo methodology, this is carried out in the model of Hovorka [23]. A similar work was performed in [37], they propose a bayesian method for the identification of a model from plasma glucose and insulin concentrations, by exploiting the prior model parameter distribution; five parameters of the UVA/Padova model was identified by this method. This contribution proposes the use of evolutionary algorithms to estimate parameters of glucose-insulin-carbohydrates dynamical models. The motivation to carry out the parametric estimation to the model of Sorensen is due to the complexity of this model, in addition, it has been used successfully in works of regulation of glucose, that is why this model is an excellent option to test new methods of identification. Evolutionary algorithms have been used in identifying parameters of biological models as it is described [41], in which a differential evolution algorithm is used to estimate the unknown parameters of a gene regulatory network model. In this manner, this contribution presents an identifiability analysis of some metabolic parameters of the model proposed by Sorensen. Such analysis is carried out using the GenSSI toolbox of MatLab® [9]. In addition a comparative analysis of the performance of the evolutionary algorithms is included.

2. IDENTIFIABILITY ANALYSIS

2.1. Compartmental model

The physiological compartmental model proposed by Sorensen is a system of 19 nonlinear ODEs. It includes three subsystems to represent the dynamics of: glucose, insulin, glucagon and metabolic rates. The complete description of the model is reported in [34]. In order to reproduce the T1DM dynamics, two assumptions are made:(see [34]): 1) the rate of release of insulin is omitted and 2) the scale of metabolic functions can be changed such that response to blood glucose levels corresponding to a patient with DMT1. The first assumption is justified because the insulin release of a T1DM patient is zero. The second concerns to the parametric identification. The complete set of equations of the Sorensen model are presented in Appendix A. To clarity in presentation, the equations are grouped together according to the subsystems they belong to: glucose (equations $(22)-(29)$), insulin (equations $(30)-(36)$), metabolic rates (equations $(37)-(54)$) and glucagon (equation (55)). Such appendix includes a brief description of the subsystems. Also, the set of nominal values of the parameters are presented in Appendix B.

2.2. Structural identifiability definition

To carry out the identifiability analysis, the Sorensen model (equation $(22)-(55)$) is rewritten as an affine system. The resulting representation is as follow:

$$\Sigma \begin{cases} \dot{x} = f(x,p) + g(x,p), x \in \mathbb{R}^n, p \in \mathbb{R}^q \\ \dot{p} = 0 \\ y = h(x), y \in \mathbb{R}^m \end{cases} \tag{1}$$

where, $x = (x_1, \cdots, x_n) \in \mathbb{R}^n$ is a measurable state vector, $p = (p_1, \cdots, p_q) \in \mathbb{R}^q$ is the unknow/uncertain parameter vector in parameter space P, $y = (y_1, \cdots, y_m) \in \mathbb{R}^m$. $f(x, p)$ is a smooth nonlinear function.

The identifiability is the property to identify the parameters of a dynamic system through its input-output behavior. Such property is a prerequisite to estimate parameters of a model uniquely from measured data [3]; thus it is necessary to know the observability properties of the model. There are different methods to analyze the observability of nonlinear systems such as system (1), the most used are the differential geometric and the algebraic approach. Rank test condition is used in both the approaches, this consists in calculate the dimension of the space spanned by gradients of the Lie-derivatives of its output functions, this defines the called observability matrix O [3]:

$$O = \begin{bmatrix} \frac{\partial h(x)}{\partial x} \\ \frac{\partial L_f h(x)}{\partial x} \\ \vdots \\ \frac{\partial L_f^{n-1} h(x)}{\partial x} \end{bmatrix} \tag{2}$$

If O is a full rank matrix ($Rank(O) = n$), then the system is algebraically observable. Parameter identifiability can be an special case of observability problem by considering parameters as state variables with null time derivative i. e., $\dot{p} = 0$, so the observability rank test can used to determine parameter identifiability. Thus, in system Σ with assumption $\dot{p} = 0$, both x and p are assumed as state variables. Assuming that the initial conditions of x are known, then x and p can be considered as non-observable variables. Suppose a full set of initial conditions on x, i. e., $x(0) = x^0$, then the problem of observability of x disappears [3]. Thus, the rank test regarding variable p in system (1) defines the following identifiability matrix:

$$O_N = \begin{bmatrix} \frac{\partial h(x)}{\partial p} \\ \frac{\partial L_f h(x)}{\partial p} \\ \vdots \\ \frac{\partial L_f^{n-1} h(x)}{\partial p} \end{bmatrix} \tag{3}$$

where $L_f h = \frac{\partial h(x)}{\partial x} f(x, p)$ is the Lie derivative [33] . Then, (1) is locally identifiable if

$$rank(O_N(p)) = q \tag{4}$$

Let us consider $p^* \in P$ and note that for all p in the neighborhood of $p^* (i.e, p \in V(p^*))$

$$y = O_N(p)p \tag{5}$$

then, condition (4) implies that for $p \in V(p^*)$:

$$p = (O_N(p)^T O_N(p))_{-1} O_N(p)^T y \tag{6}$$

Remark I. p_i, $i = 1, \ldots, q$ is a parameter estructuraly globally (or uniquely) identifiable if for almost any $p^* \in P$

$$\Sigma(p) = \Sigma(p^*) \Rightarrow p_i = p^*. \tag{7}$$

Remark II. p_i, $i = 1, \ldots, q$ is an estructuraly locally identifiable parameter if for almost any $p^* \in P$, there exists a neighbourhood $V(p^*)$ such that

$$p \in V(p^*) \text{ and } \Sigma(p) = \Sigma(p^*) \Rightarrow p_i = p^*. \tag{8}$$

Remark III. p_i, $i = 1, \ldots, q$ is an estructuraly no-identifiable parameter if for almost any $p^* \in P$, there exists no a neighbourhood $V(p^*)$ such that

$$p \in V(p^*) \text{ and } \Sigma(p) = \Sigma(p^*) \Rightarrow p_i = p^*. \tag{9}$$

A easy way to visualize the possible structural identifiability problems and to assist in the solution of the nonlinear system of equations is using of identifiability tableaus as defined in [4]. The tableau represents the non-zero elements of the jacobian of the series coefficients with respect to the parameters, and it has as many columns as parameters and as many rows as non-zero series coefficients. If the rank of the jacobian is equal to the number of parameters, then it will be possible to, at least, locally identify the parameters. When there are empty rows the rank is deficient (this may corresponds to non-identifiable parameters), or if the number of Lie derivatives is not sufficient. From the generated tableau, a number of linear independent rows are selected to guarantee the jacobian rank condition.

2.3. Numerical implementation

The numerical implementation of the structural identifiability requieres symbolic manipulation. In the special case of this contribution, the structural identifiability of de Sorensen model was carried out using the GenSSI® software [22]. This software can handle systems represented by a set of linear/nonlinear differential equations and it is based on the generating series approach coupled with the use of identifiability tableaus [4]. The underlying idea is to generate a non-linear system of equations on the parameters from the computation the successive Lie derivatives of f and g. If the solution of the system of equations is unique then the parameters are globally identifiables. Once the Lie derivatives are computed, the identifiability tableaus help not only to devise global identifiable parameters but to decide on the appropriate way to handle the non-linear system of equations on the remaining parameters.

In order to analyze the structural identifiability of Sorensen model, the system defined by equations $(22)-(55)$ is represented in state space, and considering the set of

parameters defined in Appendix B, the model can be rewritten in the affine form:

$$
\begin{aligned}
\dot{x}_1 &= p_1(x_3 - x_1) - p_2(x_1 - x_2) \\
\dot{x}_2 &= p_3(x_1 - x_2) - p_4 p_{76} \\
\dot{x}_3 &= p_5(p_6 x_1 + p_7 x_5 + p_8 x_6 + p_9 x_7 - p_{10} x_3 - p_{77}) \\
\dot{x}_4 &= p_{11}(x_3 - x_4) - p_{12} p_{78} \\
\dot{x}_5 &= p_{13}(p_{14} x_3 + p_{15} x_4 - p_{16} x_5 + (p_{59} x_{18}(p_{60} tanh(p_{61} x_{19}) - x_{17}) \times \\
&\quad (p_{62} - p_{63} tanh(p_{64}((x_5/p_{86}) - p_{65})))) - \\
&\quad (p_{69} x_{18}(p_{66} + p_{66} tanh(p_{67}((x_5/p_{86}) - p_{68}))))) \\
\dot{x}_6 &= p_{17}(x_3 - x_6) - p_{18}(p_{70} + p_{70} tanh(p_{71}(x_6 - p_{72}))) \\
\dot{x}_7 &= p_{19}(x_3 - x_7) - p_{20}(x_7 - x_8) \\
\dot{x}_8 &= p_{21}(x_7 - x_8) - p_{22}(p_{73}(x_8/p_{87})(p_{73} + p_{74} tanh(p_{75}((x_{15}/p_{88}) - p_{68})))) \\
\dot{x}_9 &= p_{23}(x_{10} - x_9) \\
\dot{x}_{10} &= p_{24}(p_{25} x_9 + p_{26} x_{12} + p_{27} x_{13} + p_{28} x_{14} - p_{19} x_{10}) \\
\dot{x}_{11} &= p_{30}(x_{10} - x_{14}) - p_{31}(x_{14} - x_{15}) \\
\dot{x}_{12} &= p_{32}(x_{10} - x_{11}) \\
\dot{x}_{13} &= p_{33}(p_{34} x_{10} + p_{35} x_{11} - p_{36} x_{12} - (p_{91}(p_{34} x_{10} + p_{35} x_{11}))) \\
\dot{x}_{14} &= p_{37}(x_{10} - x_{13}) - p_{38}(p_{92}(p_{27} x_{13})) \\
\dot{x}_{15} &= p_{39}(x_{14} - x_{15}) - p_{40}((x_{15})/((p_{90} - p_{93})/p_{93})(p_{57}) - (p_{58})) \\
\dot{x}_{16} &= p_{41}(p_{42} - p_{43} tanh(p_{44}((x_{12}/p_{45}) - p_{46})) - x_{16}) \\
\dot{x}_{17} &= p_{47}(((p_{48} tanh(p_{49} x_{19}) - p_{50})/p_{51}) - x_{17}) \\
\dot{x}_{18} &= p_{52}(p_{53} tanh((p_{54} x_{12})/p_{55}) - x_{18}) \\
\dot{x}_{19} &= p_{56}(((p_{79} - p_{80} tanh(p_{81}((x_3/p_{88}) - p_{83}))) \times \\
&\quad (p_{82} - p_{83} tanh(p_{84}((x_{10}/p_{89}) - p_{85})))) - x_{19})
\end{aligned}
\tag{10}
$$

where $x_1 = G_{BV}$, $x_2 = G_{BI}$, $x_3 = G_H$, $x_4 = G_G$, $x_5 = G_L$, $x_6 = G_K$, $x_7 = G_{PV}$, $x_8 = G_{PI}$, $x_9 = I_B$, $x_{10} = I_H$, $x_{11} = I_G$, $x_{12} = I_L$, $x_{13} = I_K$, $x_{14} = I_{PV}$, $x_{15} = I_{PI}$, $x_{16} = M_{HGP}^I$, $x_{17} = M_{HGU}^I$, $x_{18} = f_2$, $x_{19} = G_C$.

At [32] it is proved that the solutions of equations [10] are mostly sensitive to the parameters related to: the effect of glucagon in the hepatic glucose production and the effect of the glucose concentration on the hepatic glucose production. Thus, it is possible to find diverse hyperglycemia scenarios on T1DM subjects, by fitting the parameters of model $(22) - (55)$. Here, nine of the sensitive parameters reported in [32] are considered for the identifiability analysis; such parameters are: $(p_{61}, p_{62}, p_{63}, p_{64}, p_{65}, p_{73}, p_{74}, p_{75}$ and $p_{80})$. The model (10) is considered fully, that is, $y_1 = x_1$, $\dots$, $y_{19} = x_{19}$, this assumption allows us to assign values to the unknown parameters $p = [p_{61}\ p_{62}\ p_{63}\ p_{64}\ p_{65}\ p_{73}\ p_{74}\ p_{75}\ p_{80}]$.

Solution of the series approach results in an identifiability tableau of rank 9, and multiple solutions of the parameters have been found (see Figure 1). A complete solution of the parameter p_i that characterize the reduced identifiability tableu can not be found because of the computational complexity that it implies; however all parameters can be estimated.
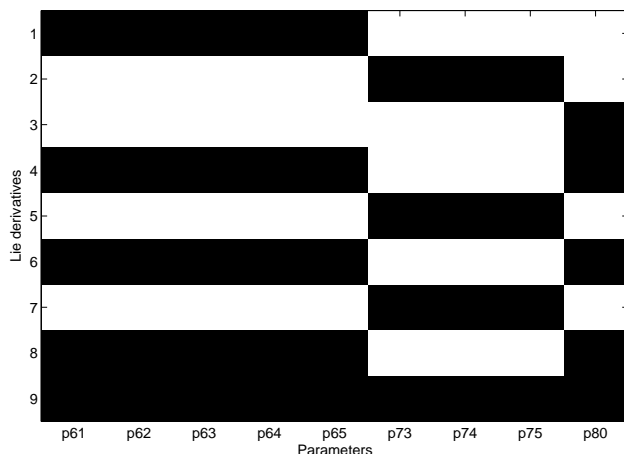
Fig. 1. First order reduced identifiability tableau obtained by means
of the generating series methods applied to the polynomial form of
the model (10).

3. PARAMETRIC ESTIMATION METHODS

Evolutionary algorithms have proven to be very effective to solve optimization problems.
In particular, the problem of parametric identification of biological models are difficult
to solve with traditional estimation techniques [41]. Thus evolutionary algorithms could
represent a useful option to solve such problem. This section provides a description of
the algorithms used for parametric identification of the Sorensen model.

3.1. Differential evolution algorithm

Differential evolution algorithm (DE) is an efficient evolutionary algorithm for global
optimization, which uses three typical operators to search the solution space: crossover,
mutation and selection [31]. DE begins with a random initialization of a population
of individuals in the search space. Therefore, it is the best overall solution using the
address information and distance according to the differentiation between populations.
However, the search behavior of each individual in the search space is set by the dynamics
of change of the address and the differentiation step.

Let be $S \subseteq \mathbb{R}^D$ the search space, DE involves a population of NP vectors (candidate
solutions):

$$x_{i,g} = [x_{1,i,g}, x_{2,i,g}, \ldots, x_{D,i,g}] \in i = 1, 2, \ldots, NP. \tag{11}$$

Mutation and crossover operator are applied to individuals in every generation g,
and a new population is generated. Then, in the selection step the individuals of both
populations compete for understanding the next generation. For each individual $x_{i,g}$,

under mutation operator, a mutant vector $v_{i,g+1} = [v_{1,i,g}, \ldots, v_{D,i,g}]$ is generated by the following equation:

$$v_{i,g} = x_{r1,g} + F(x_{r2,g} - x_{r3,g}) \tag{12}$$

where $r1, r2, r3$ belongs to $\{1, 2, \ldots, NP\}$ are randomly chosen, different among themselves and with different index i. $F \in [0, 1]$ is a constant called spreading factor which controls the amplification of the differential expansion $x_{r2,g} - x_{r3,g}$, and NP is at least four mutation. $x_{r1,g}$, the vector base, is a random member of the current population, therefore is the best information that could be shared among the population.

After the mutation, the crossover operator is applied to increase the diversification of the population. A trial vector $u_{i,g+1} = [u_{1,i,g}, \ldots, u_{D,i,g}]$ is generated by crossing the target vector $x_{i,g}$ with the corresponding mutant vector $v_{i,g}$ under a crossover rate $CR \in [0, 1]$, for every target vector $x_{i,g}$:

$$u_{j,i,g} = \begin{cases} v_{j,i,g} & \text{if } rand[0,1] \leq CR \ o \ j = randn(j) \\ x_{j,i,g} & \text{otherwise } j = 1, 2, \ldots, D \end{cases} \tag{13}$$

where rand j is the jth independent random number uniformly distributed in the range of $[0, 1]$, randn i is the index chosen randomly from the set $1, 2, \ldots, D$. $CR \in [0, 1]$ is the crossover parameter that controls the diversity of the population.

The next step is the selection, where it is decided whether the trial vector $u_{i,g+1}$ would be a member of the population of the next generation $(g + 1)$. For a minimum optimization problem, $u_{i,g+1}$ is compared to the initial target individual $x_{i,g}$ by the following selection criterion:

$$x_{i,g+1} = \begin{cases} u_{i,g}, & \text{if } f(u_{i,g}) \leq f(x_{i,g}) \\ x_{i,g}, & \text{otherwise} \end{cases} \tag{14}$$

where f is the objective function and $x_{i,g+1}$ is the individual of the new population. The procedure described above is considered as the standard version of DE. Several variants of DE have been proposed, depending on the selection of the base vector to be perturbed, the number and selection of the differentiation vectors and the type of crossover operators [31].

3.2. Ant colony algorithm

Ant colony optimization algorithm (ACO), also known as ANT, is inspired in the behavior of real colonies of ants whose are able to solve troubles of combinatorial optimization, that is, some agents works in a simple computational way and they cooperate and communicate between them using trails of artificial pheromone, this is used to identify the ways of next ants [18]. The pheromone density at real ant colonies decreases due evaporation and degradation. This effect of evaporation at the ANT is simulated with a properly defined evaporation rule. Pheromone evaporation is useful on artificial ant colonies even if it has not a noticeable effect on real ants.

In ANT, each ant is placed on different or the same corners at the beginning of the problem. The probability equation (15) determines the adyacent node of each ant at time t:

$$P_{ij}^k(t) \begin{cases} \frac{[\tau_{ij}(t)]^\alpha [\eta_{ij}(t)]^\beta}{\sum_{i \in N_i} [\tau_{ij}(t)]^\alpha \eta_{ij}(t)]^\beta}, & \text{if } k \text{ is an allowed selection} \\ 0 & , \quad \text{otherwise} \end{cases} \tag{15}$$

where $\tau_{ij}(t)$ traces amount of pheromones at (i,j) the corners, η_{ij} is the visibility value between (i,j) corners. This termn varies according to the criterium to solve the problem. α shows the relative importance of the pheromone trace in the problem. β shows the importance of the visibility value. N_i set of the node points that has not been chosen yet.

Ants make the next elections according to the probability equation. A round or iteration is completed after all the nodes at the problem have been visited. At this point, the pheromone trace is updated according to next equation [12]:

$$\tau_{ij}(t+n) = (1-\rho)\tau_{ij}(t) + \Delta\tau_{ij}(t) \tag{16}$$

ρ is the proportion of pheromone trace evaporated between the time period t and $t+1$ $(0 < \rho < 1)$. τ_{ij} stands for the pheromone trace of the corner due to the election of the (i,j) corner during a tour of the ant. This value is computed by equation (17):

$$\Delta\tau_{ij}^k(t) = \sum_{k=1}^{m} \tau_{ij} \tag{17}$$

m is total number of ants, τ_{ij}^k is the amount of pheromone trace left by the $k-$th ant at (i,j) corner. Equation (18) shows the contribute amount of the (k) ant to the pheromone trace at the (i,j) corner [1]:

$$\Delta\tau_{ij}^k = \frac{Q}{L_k} \tag{18}$$

where Q is constant, L_k is the tour length of the $k-$th ant. If the $k-$th ant used the (i,j) corner along the tour, then the trace value is calculated according to equation (18), otherwise, the trace value is zero [1].

3.3. Particle swarm optimization

Particle swarm optimization (PSO) is a population-based stochastic optimization technique proposed by Kennedy and Eberhart in [17] and [26]. PSO is easy to implement and effective to explore global solutions for some hard problems. PSO is one of the most popular optimization techniques due it has been successfully applied in many areas [28] – [38]. The concept of PSO is to simulate the social interaction behavior of birds flocking and fish schooling. PSO generates a population of particles randomly positioned in an n-dimensional search space. Each particle in the population has two vectors, one for the velocity and other for the position. During each iteration, each particle updates its velocity and position by learning from the particle's own historically best position and the best position found by the entire swarm so far. Let $V_i(v_i^1, v_i^2, \ldots, v_i^n)$ and $X_i(x_i^1, x_i^2, \ldots, x_i^n)$ be the ith particle's velocity vector and position vector, respectively, and M be the number of particles in a population. The update rules in the original PSO on the time step t, are given by:

$$v_i^j(t+1) = wv_i^j(t) + c_1 rand_1(pBest_i^j - x_i^j(t)) + c_2 rand_2(gBest_i^j - x_i^j(t)) \tag{19}$$

$$x_i^j(t+1) = x_i^j(t) + v_i^j(t) \tag{20}$$

where $pBest_i = (pBest_i^1, pBest_i^2, \ldots, pBest_i^n)$ is the historically best position of particle $i = (1, 2, \ldots, M)$, $gBest = (gBest^1, gBest^2, \ldots, gBest^n)$ is the historically best position of the entire swarm, w is the inertia factor, c_1 and c_2 are two parameters to weigh the relative importance of $pBest_i$ and $gBest$, respectively, $rand_1$ and $rand_2$ are random numbers uniformly distributed in $[0, 1]$, and $j = (1, 2, \ldots, n)$ represents the jth dimension of the search space.

4. RESULTS

4.1. Experimental data

With the goal of identify the most sensitive parameters in Sorensen model, a set of experimental data was recollected. This comes from a diabetics woman, 23 years old, with 14 year old T1DM diagnosis, 1.68m and 58.5 kg. The patient does not present any other complication or diseased associated to DM. Collected data were selected from a set of five normal days, under medical supervision, with a standard ingesta (three meals per day and some snacks) and without exercise events.

Experimental blood glucose data was recorded by a Paradigm Real-time Insulin Pump ® and Continuous Glucose Monitoring System (CGMS) by MiniMed Inc ®. Insulin pump delivers preprogrammed basal rates and preprandial bolus by subcutaneous via. This information is provided by patient in base of its particular condition, in such way, that blood glucose level will possible maintain at euglycemic range. Added to this information, patient provided to insulin pump the contents of carbohydrates for each meal. Glucose sensor is subcutaneously connected, which in turn is connected to a wireless transmitter, it provides a sample of intersticial blood glucose every five minutes to CGMS included in the insulin pump. In this way, it is possible to obtain the interaction between blood glucose level, insulin infused and meals. After lifetime of the sensor, the insulin pump and sensor should be disconnect from patient. At this moment, experimental data with blood glucose concentration, subcutaneous insulin infused and grams of carbohydrate in meals can be stored in a computer. The following data were collected for three days and sampling time of five minutes: glucose concentration, infused insulin and carbohydrates intake.

The Sorensen model considers as input the plasma insulin concentration and the continuous absorption of glucose by gut. Then these inputs must be computed from infused insulin and carbohydrate intake data via a dynamical model of subcutaneous insulin absorption and rate appearance of glucose in gut, respectively. Insulin is infused in two ways: the basal rate is a continuous infusion to support the basal metabolism whereas bolus is a single-shot infusion to correct hyperglycemia due to carbohydrate intake. Both basal rate and bolus are infused by the subcutaneous route and the corresponding plasma insulin concentration can be computed by the absorption model proposed by Berger [37]. Regarding the rate of appearance of glucose in gut, the model proposed by Lehmann is used to compute this input from carbohydrate intake data [38]. The concentration of insulin in plasma ($i(t)$) after basal and bolus doses, the rate of glucose appearance in gut (Γ_{meal}), and the glucose concentration measured by the CGMS (X_D) are shown in Figure 2.
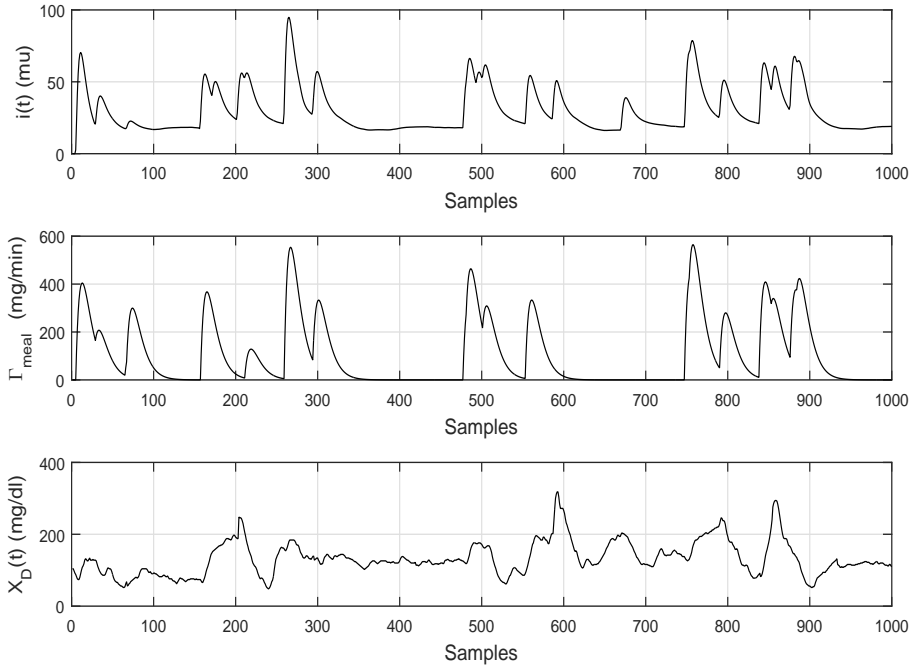
Fig. 2. Data from T1DM patient: a) Insulin concentration in plasma after bolus an basal subcutaneous dose ($i(t)$). b) Carbohydrates absorption after oral ingestion (Γ_{meal}). c) Blood glucose level concentration measured by CGMS ($X_D(t)$).

4.2. Estimation results

The data set used to estimate the sensitive parameters has been described in the previously subsection. It is observed that the dynamics of the blood glucose of Figure 2 is complex and it is difficult to faithfully reproduce such dynamics with fixed parameters. Additionally, the information that can be provided to the model is short. That is why a time window of 150 minutes (30 samples) is chosen. At this time the Sorensen model is able to reproduce a good approximation of the real dynamics of data. If the time window is decreased, the approximation would improve but the parameters would be constantly updated which could generate an overfeed. On the other hand, if the time window is increased, the approach error would increase. Considering the time window of 150 minutes, the parameters are adjusted 33 times throughout the three days of data collection. The parameter identification for the three algorithms is summarized in eight steps:

1. Set an initial interval $[t_i, t_f]$, where $t_i = 1$ and $t_f = 30$.

2. Extract a time window from the historic data X_D.

3. Estimate parameters $(p_{61}, p_{62}, p_{63}, p_{64}, p_{65}, p_{73}, p_{74}, p_{75}, p_{80})$.

4. Solve the Sorensen model (equations 22-55) from the initial time t_i until the final time t_f. Because the measured data is the interstitial glucose concentration, the state variable of the Sorensen model x_8 is considered as the output signal.

5. Compute the fitness error:

$$f_{error} = \frac{1}{n} \sum_{m=t_i}^{t_f} \sqrt{(log(x_8(m)) - log(X_D(m)))^2} \tag{21}$$

   where n represents the total data used for evaluation in the time window. $x_8(m)$ represents the glucose concentration in every time m from t_i to t_f. $X_D(m)$ stores the real concentration of blood glucose on time m.

6. If the error can not be reduced anymore go to the next step, otherwise back to the step 3.

7. To update the time window $t_i \leftarrow t_i + 30$ $t_f \leftarrow t_f + 30$.

8. If there is more data in the next time window go to step 2 otherwise end.

The numerical experiments have been performed to estimate the glucose concentration in the interstitial space of the peripheral tissue, (x_8), from the parameter sets computed by the DE, ANT and PSO algorithms. Results of each algorithm are depicted in Figure 3, Figure 4 and Figure 5, respectively. The estimation error $e(m)$ in (Figure 6) is defined as the substraction of the measure data $X_D(m)$ and the estimated one $x_8(m)$ at each sample $m = 1, \ldots, 1000$.

The experiment depicted in Figure 3 shows real data (circles) and the blood glucose concentration estimated via DE algorithm (triangles). This algorithm converges in 330 seconds; after that the error is no longer reduced or it is not reduced significantly. The total mean square error (MSE) of the experiment is 14.52236 mg/dl with a standard deviation (SD) of 9.04005 mg/dl.

In the same manner, Figure 4 and 5 show the results of estimation the blood glucose concentration from real data (circles) for ANT (triangles) and PSO (circles) algorithm, respectively. Regarding ANT algorithm, the convergence time of each estimation window was 617.78 seconds (MSE=12.02457 mg/dl, SD=7.73827 mg/dl) whereas PSO algorithm converged at 680.4 seconds (MSE=12.35 mg/dl, SD=7.91054 mg/dl). These results are summarized in Table 1.

The results show that the three algorithms have a similar estimation error. The smallest error $e(k)$ has been obtained from the ANT algorithm. DE algorithm has a short convergence time, but sacrificing the estimation error. Based on these performance criteria, the two best algorithms are PSO and ANT. Figure 7 shows a comparative graph of the blood glucose concentration estimated by both algorithms (black and blue dot-line
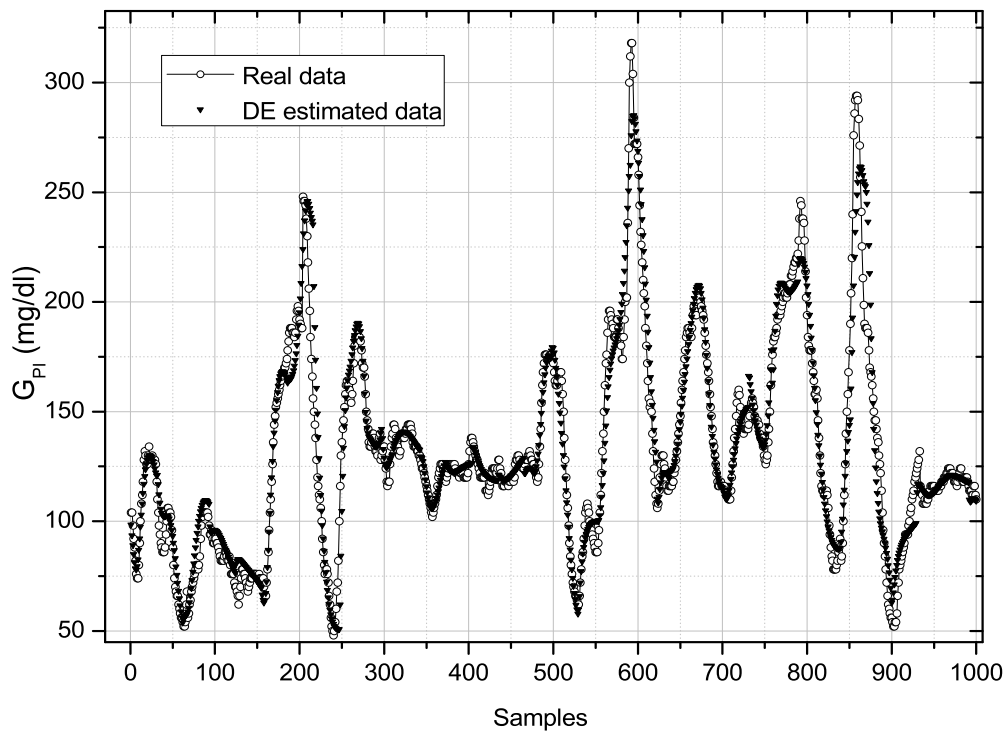
Fig. 3. Blood glucose concentration recorded by the CGMS system and the corresponding blood glucose concentration estimated by DE algorithm.

Algorithms	Convergence time (s)	MSE (mg/dl)	SD (mg/dl)
DE	330	14.52236	9.04005
ANT	617.78	12.02457	7.73827
PSO	680.40	12.35	7.91054

Tab. 1. Mean square error (MSE) and the standard deviation (SD) for each estimation algorithm.

for PSO and ANT, respectively) and the real data (red solid-line). Regarding the set of identified parameters, Table 2 summarized the mean and SD of each parameter and algorithm through the 33 time windows. It is observed that the ANT algorithm achieves a smaller SD, which means that it maintains the identified parameters in a narrow range of variation through time.
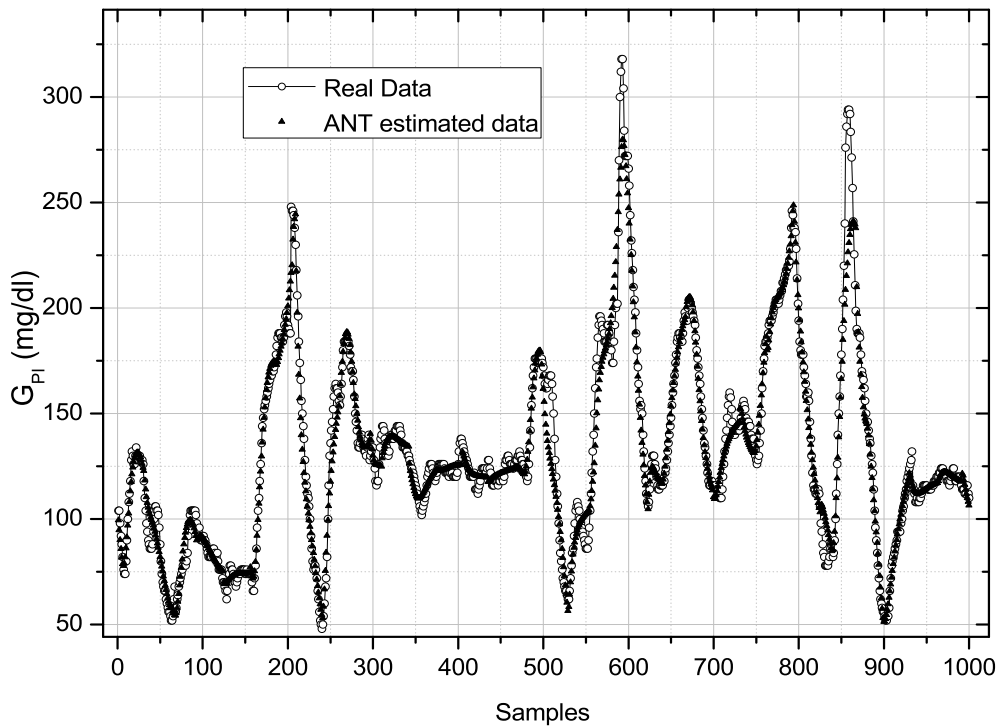
Fig. 4. Blood glucose concentration recorded by the CGMS system and the corresponding blood glucose concentration estimated by ANT algorithm.

Parameter	ANT		PSO		DE	
	Mean	SD	Mean	SD	Mean	SD
p_{61}	1.058	0.48	1.307	0.7409	1.284	0.779
p_{62}	1.7104	0.624	1.853	0.899	1.666	0.816
p_{63}	2.159	0.8301	2.211	1.105	2.136	1.162
p_{64}	1.409	0.438	1.362	0.643	1.276	0.639
p_{65}	0.809	0.585	1.135	0.8301	0.716	0.706
p_{73}	3.957	1.009	4.009	1.647	3.841	1.584
p_{74}	1.455	0.7006	1.292	1.062	1.4706	1.013
p_{75}	0.341	0.259	0.384	0.387	0.379	0.342
p_{80}	4.995	0.878	5.015	1.485	5.079	1.422

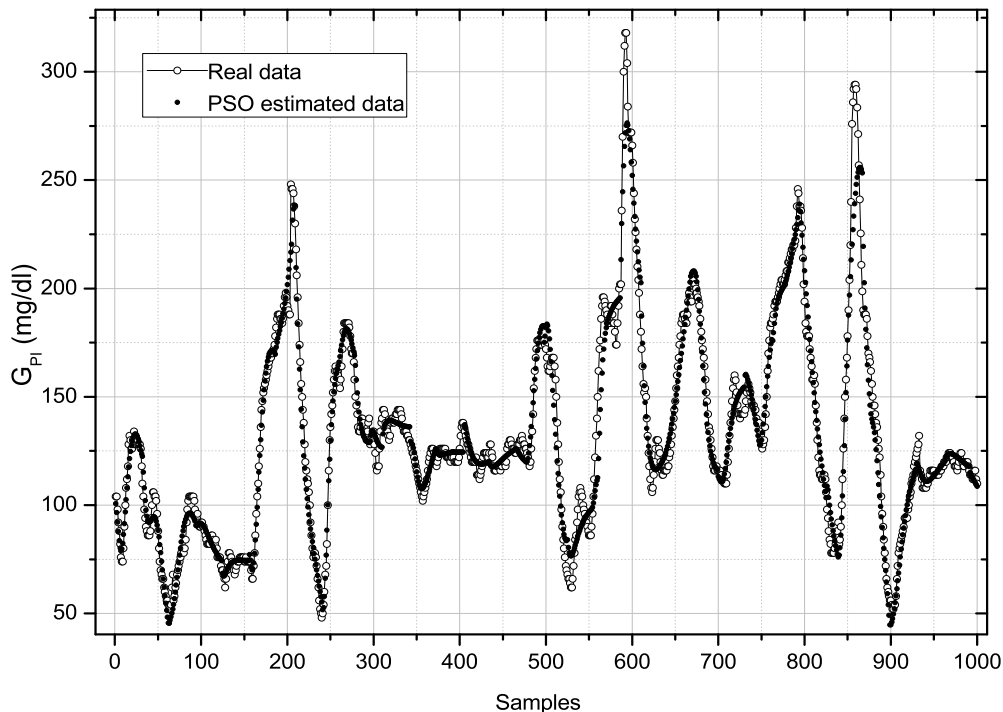**Tab. 2.** Mean and SD of the parameters identified by each algorithm.

Fig. 5. Blood glucose concentration recorded by the CGMS system
and the corresponding blood glucose concentration estimated by PSO
algorithm.

In order to analyze the behaviour of the three evolutionary algorithms presented in
this work, the wilcoxon sign-rank test was used. This is a statistical technique that uses
the fitness error of each time window in the following manner [20]. It is assumed n time
windows from a data set with two observations xi and yi for each time window i. This
results in two paired samples $x_1, \ldots, x_n$ and $y_1, \ldots, y_n$. Then $T - statistic$ is the sum
of the negative ranges obtained by $z_i = y_i - x_i$ for all $i = 1, \ldots, n$.

In this test we use the following null hypothesis.
H_0: the distribution of difference scores in two algorithms is symmetric about zero.

The critical values for the $T - statistic$ are given in the wilcoxon signed-rank table,
according to the level of significance α. The minimum level of significance for the
wilcoxon table is 0.05. In this work is used $\alpha = 0.05$ for PSO vs DE with $n = 33$,
$\alpha = 0.1$ for PSO vs ANT with n = 33 and $\alpha = 0.1$ for ANT vs DE with $n = 33$. From
this analysis it is found that $T - crit = 170$ for $\alpha = 0.5$ and $T - crit = 187$ for $\alpha = 0.1$
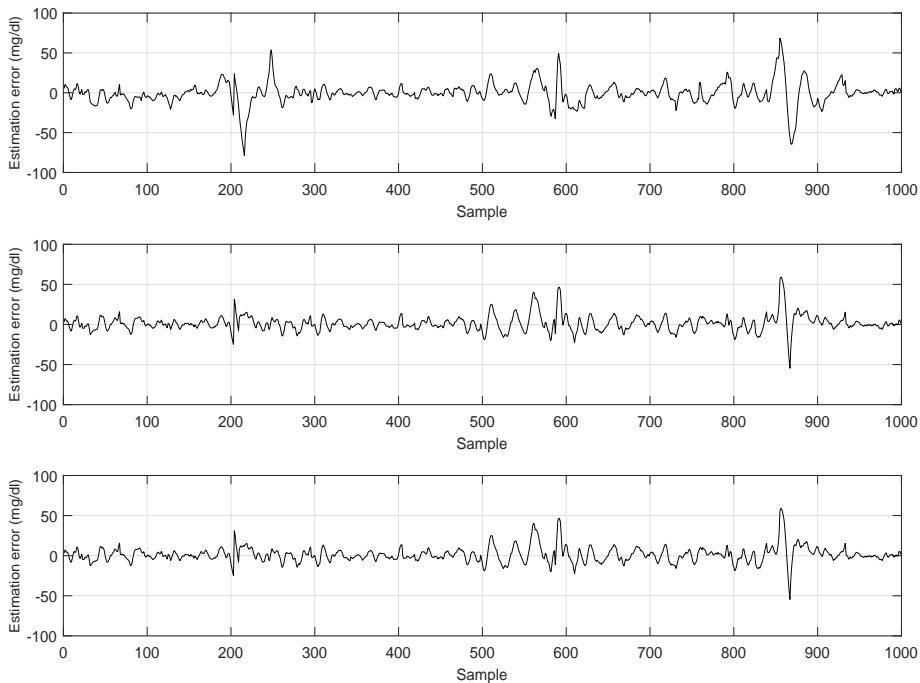(two-tail test).

Fig. 6. Estimation error of the measure data and the estimated data. Error of: DE algorithm (upper), ANT algorithm (middle) and PSO algorithm (bottom).

Since for PSO vs ANT, $T - crit = 187 < 278 = T$, we can not reject the null hypothesis, and so we can conclude that there is no significant difference between the two algorithms. For PSO vs DE, $T - crit = 170 > 166 = T$, we can reject the null hypothesis, and so we can conclude that there is a significant difference between the two algorithms. For ANT vs DE, $T - crit = 187 > 182 = T$, we can reject the null hypothesis, and so we can conclude that there is a significant difference between the two algorithms. A summary of the results are shown in the Table 3.

5. CONCLUSION

The problem of glucose regulation is a difficult task, and it depends largely of the mathematical model. This explains why many efforts have been made to mimic the dynamics of T1DM as close to reality as possible. However, in this work was considered the task of obtaining a model of the DMT1 of a single patient instead of a general model for a population. In this way, the control algorithms for glucose regulation could be
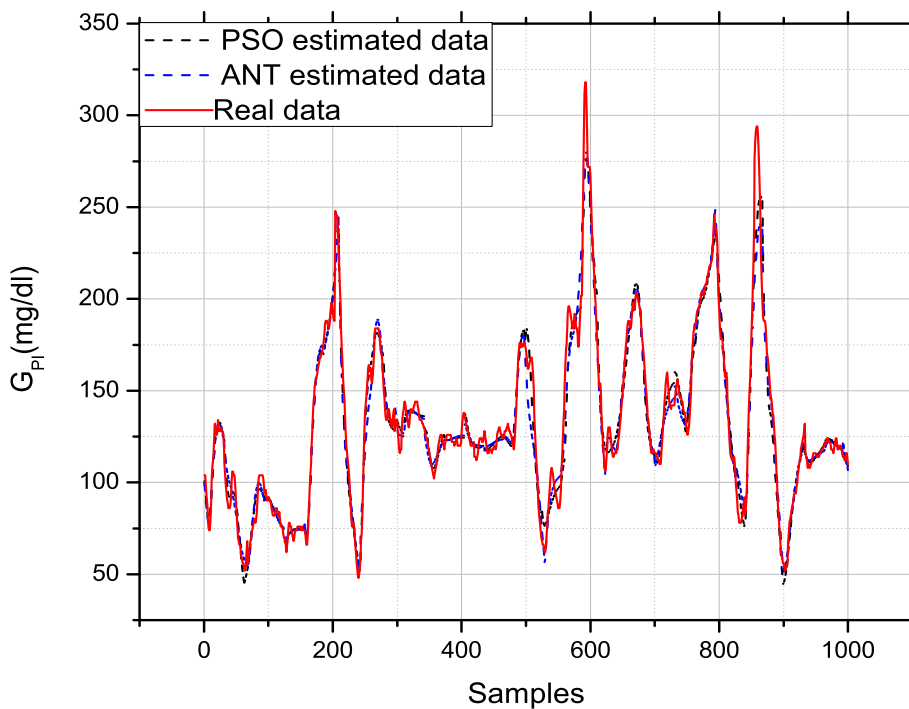
Fig. 7. Comparative graph of the blood glucose concentration estimated by both algorithms (black and blue dot-line for PSO and ANT, respectively) and the real data (red solid-line).

Parameter of test	PSO vs ANT	PSO vs DE	ANT vs DE
α	0.10	0.05	0.10
tails	2	2	2
t	278	166	182
$t - crit$	187	170	187
sig	no	si	si

Tab. 3. Parameter of wilcoxon signed-rank test.

developed according to particular conditions of a patient. Then for this purpose, the sensitive parameters play an important role in the identification of an individual model. Varying the sensitive parameters it is possible to obtain different conditions of DMT1.

In another hand, evolutionary algorithms have shown be a powerful tool in identification task. Particularly, in the case of the Sorensen model the three algorithms (ANT, DE and PSP) proved to identify successful (at least locally) the sensitive parameters. Also, the results obtained by the algorithms are close to the historical real data of the T1DM patient with an acceptable error. Although the estimation error may seem high, in fact the error that drives the glucose sensor is higher, ranging , in average, around 16.7 mg/dl and a median absolute relative differences of 13.2. This error is accepted since it is not significant and in case of control design, the error can be considered in the synthesis method in such a manner that the resulting control scheme can compensate it.

In addition, the difference between the three algorithms is acceptable. From the wilcoxon rank-test it was corroborated that ANT had a better behavior in comparison to DE. However, there is not significant difference between ANT and PSO, but it can be said that the algorithm that obtained better performance is ANT because the total MSE and SD were lower than the other two algorithms. This consideration is made such that the identification is done off-line, therefore the time of convergence is not relevant. However in terms of time DE is the one that converges in the shortest time. As future work, the model obtained can be used to test control algorithms for T1DM in-silico environment. In addition, the parameters identified can be considered as uncertain parameters, which would help to design robust controllers through the parametric variation.

A. SORENSEN MODEL

A.1. Glucose subsystem

The subsystem of glucose involves six compartments: 1) brain and central nervous system 2) heart and lungs; 3) periphery, concerns adipose tissue and skeletal muscle; 4) stomach and small intestine; 5) liver 6) kidney. The interconnection of the compartments is direct. Each compartment is a minimal required set of physiological processes to isolate the unit of glucose metabolism in organs and tissues. The mass in each compartment results in a set of eight ODE with nonlinear terms:

Brain (vascular tissue):

$$\frac{dG_{BV}}{dt} = \frac{Q_B^G}{V_{BV}^G}(G_H - G_{BV}) - \frac{V_{BI}}{V_{BV}^G T_B}(G_{BV} - G_{BI}). \qquad (22)$$

Brain (intersticial tissue):

$$\frac{dG_{BI}}{dt} = \frac{V_{BI}}{V_{BI} T_B}(G_{BV} - G_{BI}) - \frac{\Gamma_{BGU}}{V_{BI}}. \qquad (23)$$

Heart and lungs:

$$\frac{dG_H}{dt} = \frac{1}{V_H^G}(Q_B^G G_{BV} + (Q_L^G G_L + Q_K^G G_K + Q_P^G G_{PV} - Q_H^G G_H - \Gamma_{RBCU})). \qquad (24)$$

Gut:

$$\frac{dG_G}{dt} = \frac{Q_G^G}{V_G^G}(G_H - G_G) + \frac{1}{V_G^G}(\Gamma_{meal} - \Gamma_{GGU}). \qquad (25)$$

Liver:

$$\frac{dG_L}{dt} = \frac{1}{V_L^G}(Q_A^G G_H + Q_G^G G_G - Q_L^G G_L + \Gamma_{HGP} - \Gamma_{HGU}). \tag{26}$$

Kidney:

$$\frac{dG_K}{dt} = \frac{Q_K^G}{V_K^G}(G_H - G_K) - \frac{\Gamma_{KGE}}{V_K^G}. \tag{27}$$

Periphery (vascular tissue):

$$\frac{dG_{PV}}{dt} = \frac{Q_P^G}{V_{PV}^G}(G_H - G_{PV}) - \frac{V_{PI}}{T_P^G V_{PV}^G}(G_{PV} - G_{PI}). \tag{28}$$

Periphery (intersticial tissue):

$$\frac{dG_{PI}}{dt} = \frac{V_{PI}}{T_P^G V_{PI}}(G_{PV} - G_{PI}) - \frac{\Gamma_{PGU}}{V_{PI}}. \tag{29}$$

A.2. Insulin subsystem

Regarding the dynamics of insulin, it is similar to physiological glucose with the difference that this subsystem considers the pancreas as an additional compartment. This compartment is removed according to the above consideration to use it as models of T1DM. Also, the dynamics of insulin in the interstitial fluid of the brain has been overlooked, because of in the brain cell membrane is impermeable to the passage of insulin in the cerebrospinal fluid [24]:

Brain (vascular tissue):

$$\frac{dI_B}{dt} = \frac{Q_B^I}{V_B^I}(I_H - I_B). \tag{30}$$

Heart and lungs:

$$\frac{dI_H}{dt} = \frac{1}{V_H^I}(Q_B^I I_B + Q_L^I I_L + Q_K^I I_K + Q_P^I I_{PV} - Q_H^I I_H + i(t)). \tag{31}$$

Gut:

$$\frac{dI_G}{dt} = \frac{Q_G^I}{V_G^I}(I_H - I_G). \tag{32}$$

Liver:

$$\frac{dI_L}{dt} = \frac{1}{V_L^I}(Q_A^I I_H + Q_G^I I_G - Q_L^I I_L + \Gamma_{PIR} - \Gamma_{LIC}). \tag{33}$$

Kidney:

$$\frac{dI_K}{dt} = \frac{Q_K^I}{V_K^I}(I_H - I_K) - \frac{\Gamma_{KIC}}{V_K^I}. \tag{34}$$

Periphery (vascular tissue):

$$\frac{dI_{PV}}{dt} = \frac{Q_P^I}{V_{PV}^I}(I_H - I_{PV}) - \frac{V_{PI}}{T_P^I V_{PV}^I}(I_{PV} - I_{PI}). \tag{35}$$

Periphery (intersticial tissue):

$$\frac{dI_{PI}}{dt} = \frac{V_{PI}}{T_P^I V_{PI}^I}(I_{PV} - I_{PI}) - \frac{\Gamma_{PIC}}{V_{PI}}. \tag{36}$$

A.3. Metabolic rates and dynamics of glucagon

The metabolic rates (MRs) contribute in mass balance representing the physiologic processes in some compartments. In the glucose subsystem are included seven MRs. In regard insulin, three MRs are considered. In addition, there are two MRs relative for the plasma glucagon clearance rate and plasmatic glucagon release rate:

Brain glucose uptake rate:

$$\Gamma_{BGU} = 70\text{mg/min.} \tag{37}$$

Red blood cell glucose rate:

$$\Gamma_{RBCU} = 10\text{mg/min.} \tag{38}$$

Glut glucose uptake rate:

$$\Gamma_{GGU} = 20\text{mg/min.} \tag{39}$$

Periphery glucose uptake rate:

$$\Gamma_{PGU} = 35\frac{G_{PI}}{86.81}\{7.03 + 6.52tanh[0.388(\frac{I_{PI}}{5.304 - 5.82})]\}. \tag{40}$$

Hepatic glucose production rate:

$$\Gamma_{HGP} = 155M_{HGP}^I\{2.7tanh(0.39G_C) - f_2\}\left\{1.42 - 1.41tanh\left[0.62\left(\frac{G_L}{101} - 0.497\right)\right]\right\}. \tag{41}$$

Hepatic glucose production mediated by insulin:

$$\frac{d}{dt}M_{HGP}^I = \frac{1}{25}\left\{1.21 - 1.14tanh\left[2.44\left(\frac{I_L}{21.43} - 0.89\right) - M_{HGP}^I\right]\right\} \tag{42}$$

$$\frac{df_2}{dt} = \frac{1}{65}\left[\frac{2.7tanh(0.39G_C) - 1}{2} - f_2\right]. \tag{43}$$

Hepatic glucose uptake rate:

$$\Gamma_{HGU} = 20M_{HGU}^I\left\{5.66 + 5.66tanh\left[2.44\left(\frac{G_L}{101} - 1.48\right)\right]\right\}. \tag{44}$$

Solution of hepatic glucose uptake mediated by insulin:

$$\frac{d}{dt}(M_{HGU})^I = \frac{1}{25}\left[2tanh\left(0.55\frac{I_L}{21.43} - M_{HGU}^I\right)\right]. \tag{45}$$

Kidney glucose excretion rate:

$$\Gamma_{KGE} = \begin{cases} 71 + 71tanh[0.11(G_K - 460)], & 0 \leq G_K < 460 \text{mg/min} \\ -330 + 0.872G_k & , \quad G_K \geq 460 \text{mg/min}. \end{cases} \tag{46}$$

Hepatic insulin clearance rate:

$$\Gamma_{LIC} = F_{LIC}[Q_A^I I_H + Q_G^I I_G + \Gamma_{PIR}] \tag{47}$$

$$\Gamma_{LIC} = 0.40. \tag{48}$$

Pancreatic insulin release rate:

$$\Gamma_{PIR} = 0.0. \tag{49}$$

Kidney insulin clearance rate:

$$\Gamma_{KIC} = F_{KIC}[Q_K^I I_K] \tag{50}$$

$$\Gamma_{KIC} = 0.30. \tag{51}$$

Periphery insulin clearance rate:

$$\Gamma_{PIC} = \frac{I_{PI}}{\left[\left(\frac{1-F_{PIC}}{F_{PIC}}\right)\left(\frac{1}{Q_P^I}\right) - \left(\frac{T_P^I}{V_{PI}}\right)\right]} \tag{52}$$

$$\Gamma_{PIC} = 0.15. \tag{53}$$

Plasmatic glucagon release rate:

$$\Gamma_{PTR} = 2.93 - 210tanh\left[4.18\left(\frac{G_H}{91.89} - 0.61\right)\right]1.31 - 0.61tanh\left[1.06\left(\frac{I_H}{15.15 - 0.47}\right)\right]. \tag{54}$$

Only one compartment was used for modeling the counter-regulatory effect of glucagon on the glucose-insulin system.

$$\frac{d}{dt}G_C = 0.0916(\Gamma_{P\Gamma R} - G_C). \tag{55}$$

B. NOMINAL PARAMETER VALUES

$p_1 = \frac{Q_B^G}{V_{BV}^G}$ $\quad p_{11} = \frac{Q_G^G}{V_G^G}$ $\quad p_{21} = \frac{1}{T_P^G}$ $\quad p_{31} = \frac{V_{PI}}{T_P^I V_{PV}^I}$ $\quad p_{41} = \frac{1}{\tau_l}$ $\quad p_{51} = 2$

$p_2 = \frac{V_{BI}}{V_{BV}^G T_B}$ $\quad p_{12} = \frac{1}{V_G^G}$ $\quad p_{22} = \frac{1}{V_{PI}}$ $\quad p_{32} = \frac{Q_G^I}{V_G^I}$ $\quad p_{42} = 1.21$ $\quad p_{52} = \frac{1}{\tau_{GC}}$

$p_3 = \frac{1}{T_{-B}}$ $\quad p_{13} = \frac{1}{V_L^G}$ $\quad p_{23} = \frac{Q_B^I}{V_B^I}$ $\quad p_{33} = \frac{1}{V_L^I}$ $\quad p_{43} = 1.14$ $\quad p_{53} = 2$

$p_4 = \frac{1}{V_{BI}}$ $\quad p_{14} = Q_A^G$ $\quad p_{24} = \frac{1}{V_H^I}$ $\quad p_{34} = Q_A^I$ $\quad p_{44} = 1.66$ $\quad p_{54} = 0.55$

$p_5 = \frac{1}{V_H^G}$ $\quad p_{15} = Q_G^G$ $\quad p_{25} = Q_B^I$ $\quad p_{35} = Q_G^I$ $\quad p_{45} = 21.43$ $\quad p_{55} = 21.43$

$p_6 = Q_B^G$ $\quad p_{16} = Q_L^G$ $\quad p_{26} = Q_L^I$ $\quad p_{36} = Q_L^I$ $\quad p_{46} = 0.84$ $\quad p_{56} = \frac{1}{V_G^{GC}}$

$p_7 = Q_L^G$ $\quad p_{17} = \frac{Q_K^G}{V_K^G}$ $\quad p_{27} = Q_K^I$ $\quad p_{37} = \frac{Q_K^I}{V_K^I}$ $\quad p_{47} = \frac{1}{65}$ $\quad p_{57} = \frac{1}{Q_{PI}}$

$p_8 = Q_K^G$ $\quad p_{18} = \frac{1}{V_K^G}$ $\quad p_{28} = Q_P^I$ $\quad p_{38} = \frac{1}{V_K^I}$ $\quad p_{48} = 2.7$ $\quad p_{58} = \frac{T_{PI}}{V_{PII}}$

$p_9 = Q_P^G$ $\quad p_{19} = \frac{Q_P^G}{Q_{PV}^G}$ $\quad p_{29} = Q_H^I$ $\quad p_{39} = \frac{1}{T_P^I}$ $\quad p_{49} = 0.39$

$p_{10} = Q_H^G$ $\quad p_{20} = \frac{V_{PI}}{T_P^G V_{PV}^G}$ $\quad p_{30} = \frac{Q_P^I}{V_{PV}^I}$ $\quad p_{40} = \frac{1}{V_I^F}$ $\quad p_{50} = 1$

Tab. 4. Hemodynamic parameters.

$p_{59} = 155$	$p_{64} = 0.62$	$p_{69} = 20$	$p_{74} = 6.52$	$p_{79} = 2.93$	$p_{84} = 1.06$	$p_{89} = 2.55$
$p_{60} = 2.7$	$p_{65} = 0.497$	$p_{70} = 71$	$p_{75} = 0.338$	$p_{80} = 2.10$	$p_{85} = 0.47$	$p_{90} = 9.12$
$p_{61} = 0.39$	$p_{66} = 5.66$	$p_{71} = 0.11$	$p_{76} = 70$	$p_{81} = 4.18$	$p_{86} = 35.0$	
$p_{62} = 1.42$	$p_{67} = 2.44$	$p_{72} = 460$	$p_{77} = 10$	$p_{82} = 1.31$	$p_{87} = 0.0098$	
$p_{63} = 1.41$	$p_{68} = 1.48$	$p_{73} = 7.03$	$p_{78} = 20$	$p_{83} = 0.61$	$p_{88} = 5.82$	

Tab. 5. Metabolic parameters.

ACKNOWLEDGEMENT

REFERENCES

[1] K. Alaykiran, O. Engin: Karinca Kolonileri Metasezgiseli ve Gezgin Satici Problemleri Üzerinde Bir Uygulamasi. Gazi Üniv. Müh. Mim. Fak. Der. *20* (2005), 69–76.

[2] K. Alaykoran and O. Engin: The American Heritage. Dictionary of the American Language. Gazi Üniv. Müh. Mim. Fak. Der. *20* (2005), 69–76.

[3] M. Anguelova: Nonlinear Observability and Identifiability: General Theory and a Case Study of a Kinetic Model for S. cerevisiae. Department of Mathematics. Chalmers University of technology and Göteborg University SE-412 96, Göteborg 2004.

[4] E. Balsa-Canto: An iterative identification procedure for dynamic modeling of biochemical networks. BMC Systems Biology *4* (2010), 1, 4–11. DOI:10.1186/1752-0509-4-11

[5] M. Berger and D. Rodbard: Computer simulation of plasma insulin and glucose dynamics after subcutaneous insulin injection. Diabetes Care *12* (1989), 10, 725–736. DOI:10.2337/diacare.12.10.725

[6] R. N. Bergman, Y. Z. Ider, C. R. Bowden, and C. Cobelli: Quantitative estimation of insulin sensitivity. Amer. J. Physiology *236* (1979), 6, E667–E677.

[7] F. Chee and T. Fernando: Closed-Loop Control of Blood Glucose. Springer *368*, Berlin, Heidlberg 2007. DOI:10.1007/978-3-540-74031-5

[8] O. T. Chis, J. R. Banga, and E. Balsa-Canto: Structural identifiability of systems biology models: A critical comparison of methods. PLos One *6* (2011), 11, e27755. DOI:10.1371/journal.pone.0027755

[9] O. Chis, J. R. Banga and E. Balsa-Canto: GenSSI: a software toolbox for structural identifiability analysis of biological models. Bioinformatics *27* (2011), 18, 2610–2611. DOI:10.1093/bioinformatics/btr431

[10] C. Cobelli, C. Dalla Man, G. Sparacino, L. Magni, G. de Nicolao, and B. Kovatchev: Models, signals and control (Methodological review). IEEE Rev. Biomed. Engrg. *2* (2009), 54–96. DOI:10.1109/rbme.2009.2036073

[11] P. Colmegna and R. S. Sanchez Peña: Analysis of three T1DM simulation models for evaluating robust closed-loop controllers. Computer Methods and Programs in Biomedicine *113* (2014), 371–382. DOI:10.1016/j.cmpb.2013.09.020

[12] A. Colorni, M. Dorigo, and V. Maniezzo: Distributed Optimization by Ant Colonies. In: The First European Conference on Artificial Life. Paris 1992.

[13] T. K. Das, G. K. Venayagamoorthy, and U. O. Aliyu: Bio-inspired algorithms for the design of multiple optimal power system stabilizers: SPPSO and BFA. IEEE Trans. Ind. Appl. *44* (2008), 5, 1445–1457. DOI:10.1109/tia.2008.2002171

[14] H. Davson and E. Spaziani: The bloodbrain barrier and the extracellular space of the brain. J. Physiology *149* (1959), 1, 135–143. DOI:10.1113/jphysiol.1959.sp006330

[15] Y. del Valle, G. K. Venayagamoorthy, S. Mohagheghi, J.-C. Hernandez, and R. G. Harley: Particle swarm optimization: Basic concepts, variants and applications in power systems. IEEE Trans. Evol. Comput. *12* (2008), 2, 171–195. DOI:10.1109/tevc.2007.896686

[16] S.-R. Dikondwar: Design and development of insulin delivery system prototype. In: Communication Software and Networks (ICCSN), IEEE 3rd International Conference 2011, pp. 575–579. DOI:10.1109/iccsn.2011.6014636

[17] R. C. Eberhart and J. Kennedy: A new optimizer using particle swarm theory. In: Proc. 6th Int. Symp. Micromachine Hum. Sci. 1995, pp. 39–43.

[18] T. Ergüzel and E. Akbay: ACO (Ant Colony Optimization) Algoritmasi ile Yrnge Takibi. Izmit, Kocaeli 2007.

[19] R. Femat, E. Ruiz-Velázquez, and G. Quiroz: Weighting restriction for intravenous insulin delivery on t1dm patient via H_∞ control. IEEE Trans. Automat. Sci. Engrg. *6* (2009), 2, 239–247. DOI:10.1109/tase.2008.2009089

[20] S. Garcia, D. Molina, M. Lozano, and F. Herrera: A study on the use of non-parametric tests for analyzing the evolutionary algorithms behaviour: A case study on the CEC'2005 Special Session on Real Parameter Optimization. Springer Science Business Media, J Heuristics *15* (2008), 617–644. DOI:10.1007/s10732-008-9080-4

[21] E. J. Gómez and M. E. Hernando Pérez y Thomas: The INCA system: A further step towards a telemedical artificial pancreas. IEEE Trans. Inform. Technol. Biomedicine *12* (2008), 4, 470–479. DOI:10.1109/titb.2007.902162

[22] J. R. Guyton: A model of glucose-insulin homeostasis in man that incorporates the heterogeneous fast pool theory of pancreatic insulin realise. Diabetes (1978), 1027–1042. DOI:10.2337/diabetes.27.10.1027

[23] A. Haidar, E. M. Wilinska, J. A. Graveston, and R. Hovorka: Stochastic virtual population of subjects with type 1 diabetes for the assessment of closed-loop glucose controllers. IEEE Trans. Biomed. Engrg. *60* (2013), 12, 3524–3533. DOI:10.1109/tbme.2013.2272736

[24] R. A. Harvey, Y. Wang, B. Grosman, M. W. Percival, W. Bevier, D. A. Finan, H. Zisser, D. E. Sebong, L. Jovanovic, F. J. Doyle III, and E. Dassau: Quest for the artificial pancreas: combining technology with treatment. In: IEEE Engrg. Medicine Biol. Magazine *29* (2010), 2, 53–62. DOI:10.1109/memb.2009.935711

[25] R. Hovorka, F. Shojaee-Moradie, P. V. Carroll, L. J. Chassin, I. J. Gowrie, N. C. Jackson, R. S. Tudor, A. M. Umpleby, and R. H. Jones: Partitioning glucose distribution/transport, disposal, and endogenous production during ivgtt. Amer. J. Physiol. Endocrinol. Metabol. *282* (2002), 5, E992-E1007. DOI:10.1152/ajpendo.00304.2001

[26] J. Kennedy and R. C. Eberhart: Particle swarm optimization. In: Proc. IEEE Int. Conf. Neural Netw. 1995, pp. 1942–1948. DOI:10.1109/icnn.1995.488968

[27] E. D. Lehmann and T. Deutsch: Physiological model of glucose-insulin interaction in type I diabetes mellitus. J. Biomedical Engrg. *14* (1992), 235–242. DOI:10.1016/0141-5425(92)90058-s

[28] H. S. Lin, W. H. Liauh, and S. J. Ho: OPSO: Orthogonal particle swarm optimization and its application to task assignment problems. IEEE Trans. Syst. Man Cybern. B *38* (2008), 2, 288–289. DOI:10.1109/tsmca.2007.914796

[29] C. Man, R. Rizza and Cobelli: Meal simulation model of the glucose-insulin system. IEEE Trans. Biomed. Engrg. *54* (2007), 10, 1740–1749. DOI:10.1109/tbme.2007.893506

[30] M. G. Pedersen, G. M. Toffolo, and Cobelli: Cellular modeling: insight into oral minimal models of insulin secretion. Amer. J. Physiol. Endocrinol. Metabol. *298* (2010), E597–E601. DOI:10.1152/ajpendo.00670.2009

[31] B. Peng, B. Liu, F. Zhang, and L. Wang: Differential evolution algorithm-based parameter estimation for chaotic systems. Chaos, Solitons Fractals *39* (2009), 2110–2118. DOI:10.1016/j.chaos.2007.06.084

[32] G. Quiroz and R. Femat: On hyperglicemic glucose basal levels in Type 1 Diabetes Mellitus from dynamic analysis.   Math. Biosciences *210* (2007), 554–575. DOI:10.1016/j.mbs.2007.06.004

[33] W. Respondek: Geometry of static and dynamic feedback. In: Lectures given at the Summer School on Mathematics Control Theory, Trieste 2001 and Bedlewo-Warsaw 2002, Laboratoire de Mathématiques INSA, Rouen.

[34] J. T. Sorensen: A Physiology Model of Glucose Metabolism in Man And Its Use to Design and Asses Improved Insulin Therapies for Diabetes. Ph.D. Dissertation, Massachusetts Institute of Technology 1985.

[35] J. Tiran, K. R. Galle, and Jr. Porte: A simulation model of extracellular glucose distribution in the human body.   Ann. Biomedical Engrg. *3* (1975), 34–46. DOI:10.1007/bf02584487

[36] B. Tuch, M. Dunlop and J. Proietto. Diabetes Research: A guide for Postgraduates. Taylor and Francis e-Library, 2004.

[37] R. Visentin, C. Dalla Man, and C. Cobelli: One-day Bayesian cloning of type 1 diabetes subjects: Toward a single-day UVA/Padova type 1 diabetes simulator. IEEE Trans. Biomed. Engrg. *63* (2016), 11, 2416–2424. DOI:10.1109/tbme.2016.2535241

[38] M. P. Wachowiak, R. Smolikova, Y. Zheng, J. M. Zurada, and A. S. Elmaghraby: An approach to multimodal biomedical image registration utilizing particle swarm optimization multimodal function optimization based on particle swarm optimization. IEEE Trans. Evol. Comput. *8* (2004), 3, 289–301. DOI:10.1109/tevc.2004.826068

[39] M. E. Wilinska and R. Hovorka: Simulation models for in silico testing of closed-loop glucose controllers in type 1 diabetes. Drug Discov, Today Dis. *5* (2008), 289–298. DOI:10.1016/j.ddmod.2009.07.005

[40] World Health Organization: Global Report in Diabetes. Printed in France, 2016.

[41] C. Zhan, W. Situ, L. Fat Yeung, P. Wai-Ming Tsang, and G. YANG: A parameter estimation method for biological systems modeled by ODEs/DDEs models using spline approximation and differential evolution algorithm. IEEE Trans. Computat. Biology Biomath. *11* (2014), 1066–1076. DOI:10.1109/tcbb.2014.2322360

Eduardo Ruiz Velázquez, Universidad de Guadalajara, Boulevard Gral. Marcelino García Barragán 1421, Guadalajara, Jalisco. México.
e-mail: eduardo.ruiz@cucei.udg.mx

Oscar D. Sánchez, Universidad de Guadalajara, Boulevard Gral. Marcelino García Barragán 1421, Guadalajara, Jalisco. México.
e-mail: oscardidiersanchez@gmail.com

Griselda Quiroz, Universidad Autónoma de Nuevo León, UANL, FIME Avenida Universidad S/N, Ciudad Universitaria, 66455, San Nicolás de los Garza, Nuevo León, N.L. México.
e-mail: griselda.quirozcm@uanl.edu.mx

Guillermo O. Pulido, Universidad de Guadalajara, Boulevard Gral. Marcelino García Barragán 1421, Guadalajara, Jalisco. México.
e-mail: guillermo.obregon@cucei.udg.mx